A Special Higher Order Finite-Element Method for Scattering by Deep Cavities

Jian Liu and Jian-Ming Jin, *Senior Member, IEEE*

***Abstract*—A special higher order finite-element method is presented for the analysis of electromagnetic scattering from a large, deep, and arbitrarily shaped open cavity. This method exploits the unique features of the finite-element equations and, more importantly, the unique features of the problem of scattering by a large and deep cavity. It is designed in such a manner that it uses minimal memory, which is proportional to the maximum cross section of the cavity and independent of the depth of the cavity, and its computation time increases only linearly with the depth of the cavity. Furthermore, it computes the scattered fields for all angles of incidence without requiring significant additional time. The technique is implemented with higher order tetrahedral and mixed-order prism elements, both having curved sides to allow for accurate modeling of arbitrary geometries. Numerical results show that higher order elements yield a remarkably more accurate and efficient solution for scattering by three-dimensional (3-D) cavities. Of the two kinds of element, the mixed-order prism is optimal for the proposed special solver.**

***Index Terms*—Cavities, electromagnetic scattering, finite-element method.**

I. Introduction

NUMERICAL computation of the radar cross section (RCS) of a deep open cavity is considered a grand challenge in computational electromagnetics (CEM). When a cavity is very large compared to the wavelength and its interior geometry is simple, high-frequency asymptotic techniques based on ray tracing and edge diffraction can be employed to evaluate its RCS [1]–[9]. These include the shooting-and-bouncing-ray (SBR) method, the Gaussian beam shooting method, the generalized ray expansion (GRE) method, and the iterative physical optics (IPO) method. When a cavity is small, numerical techniques such as the method of moments (MoM), the finite-element method (FEM), and their combination can be applied for the calculation of the RCS [10]–[20]. These methods can accurately model arbitrarily shaped cavities as well as the complex structures inside cavities. However, the computational costs (memory and CPU time) to model a large cavity can exceed even the most powerful supercomputer. When a cavity has a special cross section (rectangular or circular) with a planar termination, the waveguide modal approach is an efficient method over a broad range of frequencies [21]–[25] (The modal approach can also be applied to cavities having an arbitrary cross section whose waveguide modes are calculated using the FEM [26]). In addition to the aforementioned techniques, a variety of hybrid techniques combining a high frequency and a numerical method have also been proposed to solve the cavity scattering problems [27]–[30]. These hybrid techniques are intended to reduce the size of the computational domain for the numerical method and thus increase the efficiency and capability of their solutions. However, the size of a cavity is still limited by the memory and CPU time required by the numerical method.

Recently, a very efficient numerical technique is developed for the analysis of electromagnetic scattering from a large, deep, and arbitrarily shaped cavity [31]. This technique is based on the FEM that is known for its capability to handle arbitrary geometries and complex material composition. The FEM mesh at the cavity aperture is terminated in an exact manner by the boundary-integral (BI) method. The technique exploits the unique features of the FE-BI equations and, more importantly, the unique features of the problem of scattering by a large and deep cavity. It is designed in such a manner that it uses minimal memory, which is proportional to the maximum cross section of the cavity and independent of the depth of the cavity, and its computation time increases only linearly with the depth of the cavity. Furthermore, it computes the scattered fields for all angles of incidence without requiring significant additional time. The technique has been applied to both two-dimensional (2-D) and simple three-dimensional (3-D) cavities whose interior surfaces may be coated with radar absorbing materials (RAM). Excellent results are obtained for 2-D cavities and those for 3-D cavities are also promising. The 3-D implementation used the zeroth-order rectangular brick elements [31] and later the zeroth-order tetrahedral elements, which are commonly known as edge elements. It was observed that the solution accuracy was mostly limited by the dispersion error of the zeroth-order elements. This error increases with the size of the FEM region and can be devastating when the FEM region is large [32]. Hence, the size of a 3-D cavity to be analyzed by the proposed method is mainly limited by the use of the zeroth-order elements.

In this paper, we enhance the efficiency and capability of the special technique using higher order curvilinear elements. The use of these higher order elements significantly reduces the dispersion error and also permits more accurate modeling of the problem geometry. We first implement the special technique using higher order vector isoparametric tetrahedral elements. It is shown that these elements yield a remarkably more accurate and efficient solution. However, the improvement of the efficiency is limited by the nature of the special technique. We then

Manuscript received September 22, 1999; revised December 16, 1999. This work was supported by a grant from AFOSR via the MURI Program under Contract F49620-96-1-0025.

The authors are with the Center for Computational Electromagnetics, Department of Electrical and Computer Engineering, University of Illinois at Urbana-Champaign, Urbana, Illinois 61801-2991 USA.

Publisher Item Identifier S 0018-926X(00)04382-9.

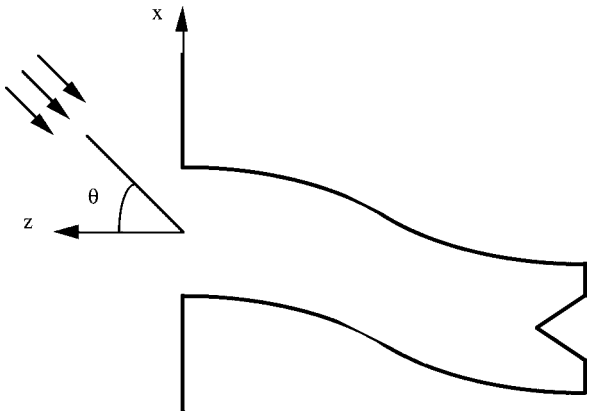

Fig. 1. Illustration of a large, deep, and arbitrarily shaped open cavity.

develop mixed-order prism elements, which are proven to be optimal for the special solver. Numerical examples show that the proposed special FEM is a very promising technique for the simulation of scattering by a large, deep, and arbitrarily shaped open cavity.

II. Method

Consider the problem of plane wave scattering by a large, deep, and arbitrarily-shaped open cavity (Fig. 1). In accordance with the finite-element and boundary-integral (FE-BI) method [33], the electric field inside the cavity and at the aperture of the cavity can be obtained by seeking the stationary point of the functional

$$\begin{aligned} F = \frac{1}{2}\iiint_V \left[\frac{1}{\mu_r}(\nabla\times\mathbf{E})\cdot(\nabla\times\mathbf{E}) - k^2\epsilon_r\mathbf{E}\cdot\mathbf{E}\right] dV \\ - k^2\iint_S \mathbf{M}(\mathbf{r})\cdot\left[\iint_S \mathbf{M}(\mathbf{r}')G(\mathbf{r},\mathbf{r}')\,dS'\right] dS \\ + \iint_S \nabla\cdot\mathbf{M}(\mathbf{r})\left[\iint_S G(\mathbf{r},\mathbf{r}')\nabla'\cdot\mathbf{M}(\mathbf{r}')\,dS'\right] dS \\ - 2jkZ\iint_S \mathbf{M}(\mathbf{r})\cdot\mathbf{H}^{\text{inc}}(\mathbf{r})\,dS \end{aligned} \tag{1}$$

where V denotes the volume of the cavity and S denotes its aperture, $\mathbf{M} = \mathbf{E}\times\hat{z}$ is the equivalent magnetic current over the aperture, $\mathbf{H}^{\text{inc}}$ denotes the incident magnetic field, k is the free-space wavenumber, Z is the free-space wave impedance, and $G(\mathbf{r},\mathbf{r}')$ denotes the free-space Green's function.

This functional can be discretized by first subdividing the volume of the cavity into small tetrahedral or triangular prism elements and then representing the field as

$$\mathbf{E} = \sum_{i=1}^{N} E_i\mathbf{N}_i \tag{2}$$

where $\mathbf{N}_i$ denotes the vector basis function, E_i denotes the expansion coefficient, and N denotes the total number of expansion terms. In this work, we employ higher order interpolatory vector basis functions discussed in Sections IV and V.

Substituting (2) into (1) and applying the Rayleigh–Ritz procedure, we obtain the matrix equation

$$[A]\{E\} = \{b\} \tag{3}$$

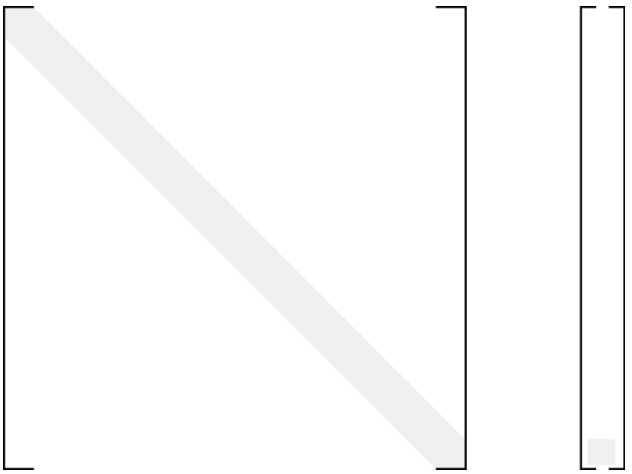

Fig. 2. (a) The structure of the finite-element matrix, whose nonzero elements are contained within a narrow band. (b) The structure of the right-hand side vector, which contains a very few nonzero elements at the bottom of the vector.

where $[A]$ is a symmetric matrix, $\{E\}$ is a vector storing the discrete unknowns, and $\{b\}$ is a known vector determined from the incident field. The matrix $[A]$ is contributed by the first three integrals in (1) and can be decomposed into two parts: the part contributed by the volume integral is sparse and the other part contributed by the two surface integrals is fully populated. The problem is to solve (3) for $\{E\}$ from which the electric field can be calculated using (2).

Although the formulation of the FEM matrix equation is straightforward, its solution is difficult because of a large number of unknowns for a large and deep cavity. To illustrate this difficulty, consider a circular cavity with a diameter of five wavelengths and a depth of 50 wavelengths. If we use 20 zeroth-order elements per wavelength, we would have about 1000 layers along the depth of the cavity with about 24 000 unknowns per layer, resulting in 24 million unknowns. Clearly, for a problem of this size, the most important factor for its numerical solution is the memory requirement.

The most memory-efficient method to solve (3) is an iterative method such as the conjugate gradient (CG), the biconjugate gradient (BCG), and the quasiminimum residual (QMR) methods. Using such a method, the memory requirement is proportional to $O(N)$. For the cavity considered here, the memory required is estimated to be about 7.68 Gb. However, an iterative method for this problem has two major problems. The most serious problem is its slow or nonconvergence. Since the finite-element matrix has a relatively poor condition, when its dimension is large the convergence of an iterative solution is very slow and, in most cases that we have tested, the solution even fails to converge. Although the slow convergence can be improved using a preconditioning technique, its implementation requires a large amount of memory, usually exceeding that for the storage of $[A]$. The less serious, but also important, problem is that an iterative method must repeat the entire solution process for a new right-hand side. Since we are interested in the RCS calculation, the number of right-hand sides can be very large.

It is well known that a direct method can find the solution of a matrix equation with a fixed number of operations and, more-

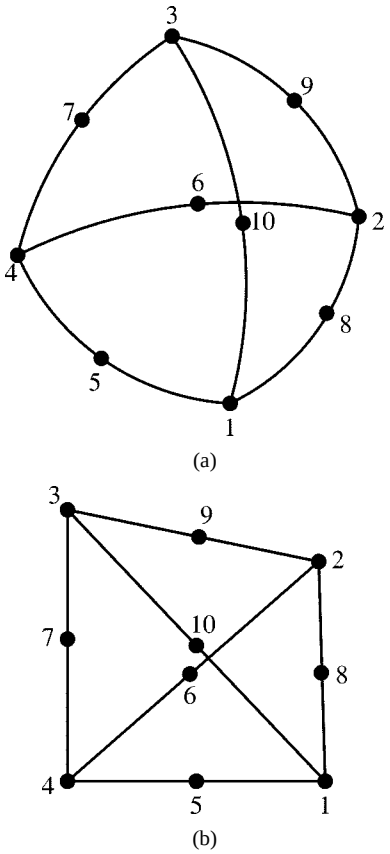

Fig. 3. A second-order tetrahedral element. (a) Curved element. (b) Rectilinear element.

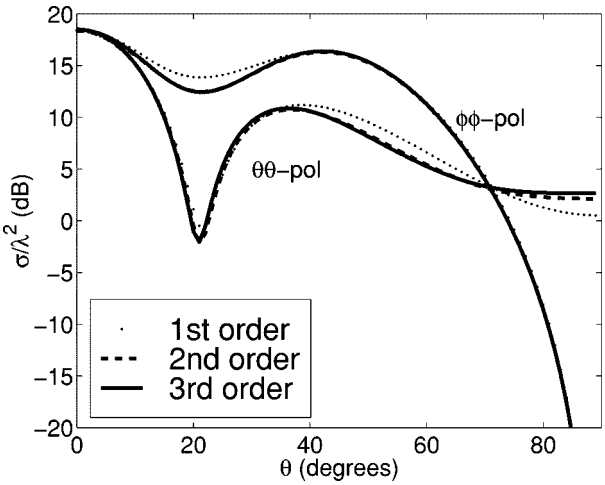

Fig. 4. Monostatic RCS of a $1.5\lambda \times 1.5\lambda \times 0.6\lambda$ rectangular cavity modeled with tetrahedral elements.

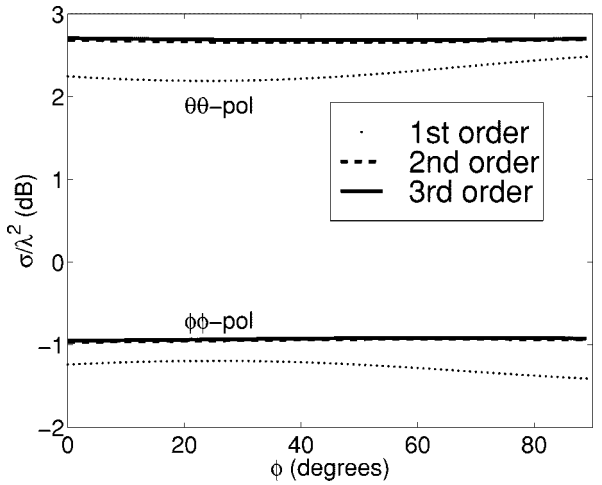

Fig. 5. Monostatic RCS of a circular cavity having a diameter of 0.61λ and depth of 2.1λ modeled with tetrahedral elements. $\theta = 40°$.

over, it can find the solution for many right-hand sides with a negligible amount of extra computing time. Therefore, it seems that a direct method is preferred for this problem. However, the major problem for a direct method is its huge memory requirement. For the cavity considered here, with a proper numbering of the unknowns, the matrix $[A]$ can be stored in a banded matrix whose half bandwidth is about 24 000. This would require 4608 Gb, which far exceeds the capability of most available computing facilities.

From the above analysis, it is clear that one must reduce the memory requirement to render a direct method useful for a large problem. In general, this is impossible; however, the problem considered here possesses several unique features that make this reduction possible. If we number the unknowns starting from the bottom of the cavity, we obtain the matrix $[A]$ with two very unique features (Fig. 2). First, $[A]$ is a symmetric and banded matrix, which is mostly sparse except for the right-bottom part that is a full matrix generated from the first two surface integrals in (1). The half bandwidth is approximately equal to the number of unknowns for one layer. For the cavity considered here, it is about 24 000. Second, $\{b\}$ is a vector whose elements are zeros except for a small part at the bottom, which is contributed by the last surface integral in (1). For the cavity considered here, out of 24 million elements in $\{b\}$, only 24 000 of them are nonzeros and they are at the bottom of $\{b\}$. Recognizing these two unique features, we can design a special method to solve (3) efficiently.

This special method is based on the band solver. As pointed out above, a band solver for a general problem would require the storage of the banded matrix, which requires about 4608 Gb for the cavity considered here. However, a careful examination of the Gaussian elimination process reveals that for a symmetric banded matrix having a half bandwidth of iwb, the elimination of an equation only involves the previous iwb equations. Other equations preceding these iwb equations are never needed in the elimination process; they are needed only in the back-substitution process. Since again $\{b\}$ is nonzero only at its bottom and the calculation of RCS requires only the electric field at the aperture of the cavity, these equations are actually never needed after the elimination process. Recognizing this fact, we can modify the band algorithm in such a manner that only a matrix of $iwb \times iwb$ is needed for its implementation. For the cavity considered here, the memory required is about 4.6 Gb. In this modified band algorithm, we begin with the first equation and generate the equations one by one. Once an equation is generated, we immediately apply Gaussian elimination to this equation and keep the reduced equation in the memory. This process continues until we encounter the $(iwb+1)$th equation. Since the first equation is not needed in the Gaussian elimination of this equation, we place this equation in the memory occupied by the

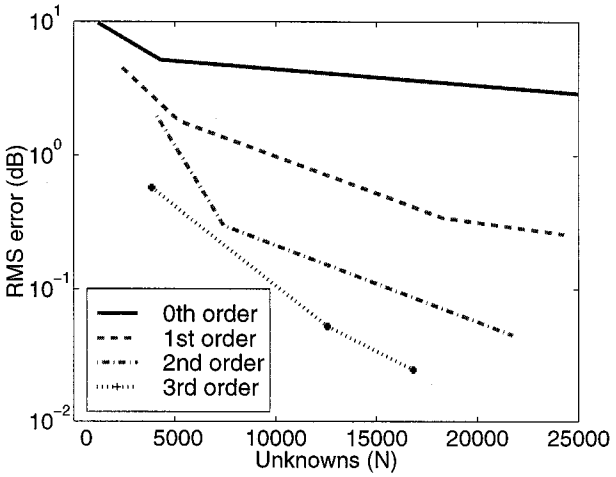

(a)

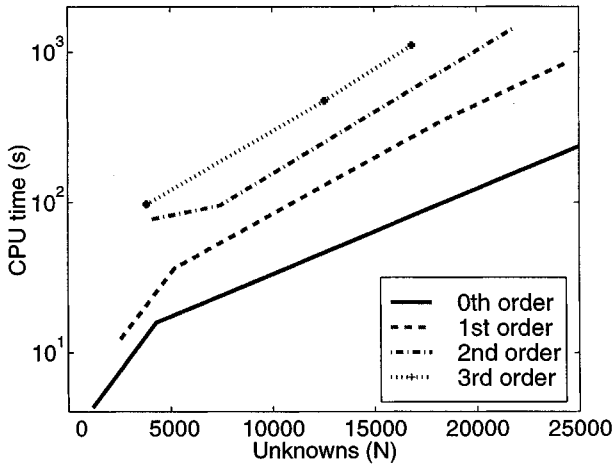

(b)

Fig. 6. (a) RMS error versus the number of unknowns for the monostatic RCS of a 1.0 λ $\times$ 1.0 λ $\times$ 4.0 λ rectangular cavity modeled with tetrahedral elements. (b) Corresponding CPU time.

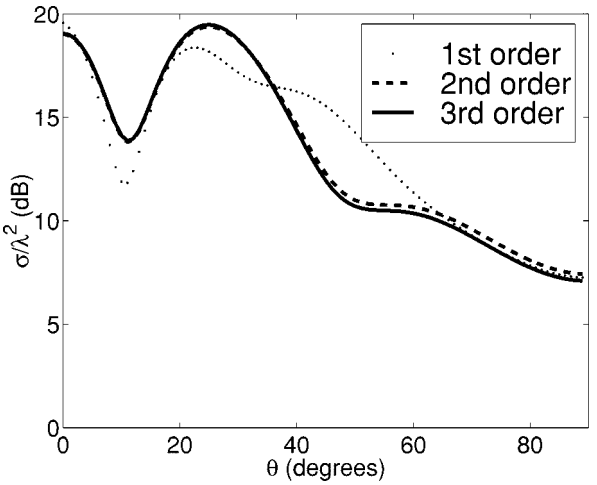

(a)

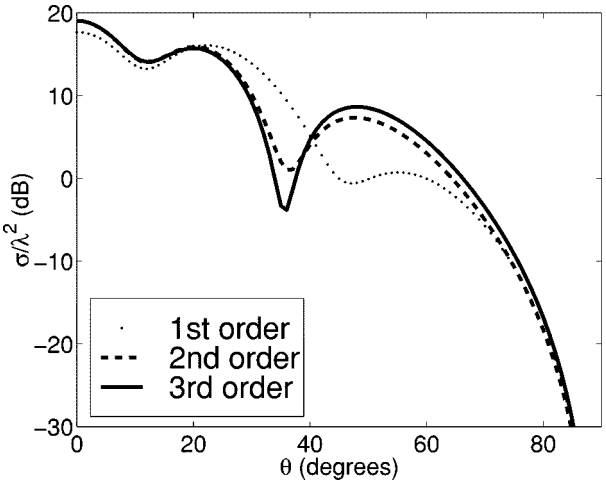

(b)

Fig. 7. Monostatic RCS of a circular cavity having a diameter of 2.0λ and depth of 10.0λ modeled with tetrahedral elements. (a) $\theta\theta$ polarization. (b) $\phi\phi$ polarization.

first equation. This process continues until all the equations have been processed. The information remaining in the core memory is all that is needed to find the solution of the unknowns at the aperture of the cavity via the back substitution process.

III. Computational Complexity

In order to design an efficient method, it is important to understand the computational complexity of the proposed special algorithm. A straightforward analysis shows that this algorithm has the computing time proportional to $(iwb)^2N$ and memory requirement proportional to $(iwb)^2$, where N is the total number of unknowns. Since iwb is determined by the maximum cross section of a cavity and N is linearly proportional to the depth of a cavity, it follows that the memory requirement of the algorithm is proportional to the maximum cross section of the cavity and independent of the depth of the cavity and its computing time increases only linearly with the depth of the cavity.

We first implemented this method using the zeroth-order vector tetrahedral elements, which are commonly known as the edge elements. Although we obtained excellent results for small cavities, we found that its capability for large 3-D cavities is limited. This limitation is mainly due to the dispersion error of the zeroth-order elements, which accumulates during wave propagation. As a result, the total error increases with the size of the FEM region [32]. A simple approach to reducing the dispersion error is to decrease the element size or increase the mesh density. However, the computational complexity indicates that for a fixed-size cavity using the zeroth-order elements, the memory requirement scales as D^4 and the computing time scales as D^7, where D denotes the mesh density (number of unknowns per wavelength). Therefore, an increase of the mesh density by a factor of two can increase the memory requirement by a factor of 16 and the computing time by a factor of 128 and an increase of the mesh density by a factor of three can increase the memory requirement by a factor of 81 and the computing time by a factor of 2187. Our numerical experiments indicated that for a large and deep cavity, it typically requires the mesh density above 40 points per wavelength for the zeroth-order elements. Hence, the quick increase in the memory requirement and computing time is devastating for the analysis of large and deep cavities.

TABLE I
INFORMATION ABOUT RCS CALCULATION OF A CIRCULAR CAVITY

Order of Elements	Number of Unknowns	Memory (MB)	CPU Time (s)
First	14,218	6.8	381
Second	42,555	21.5	9,985
Third	94,844	77.9	89,435

The simple analysis performed above reveals the limitation of the zeroth-order elements and leads us to the use of higher order elements. It is well known that the higher order elements can significantly reduce the dispersion error and permit a lower mesh density. When higher order tetrahedral elements are used, for a fixed-size cavity the memory requirement scales as $(p+1)^2D^4$ and the computing time scales as $(p+1)^2D^7$, where p denotes the order of the elements. Although there is an additional coefficient $(p+1)^2$ in both the memory requirement and computing time, the higher order elements use a much lower mesh density D, which can lead to a significant saving in the memory and computing time.

IV. HIGHER ORDER TETRAHEDRAL ELEMENTS

For the FEM analysis, the cavity volume is first subdivided into small tetrahedral elements. These elements can have curved sides in order to model the cavity geometry accurately. Each curved tetrahedron is then transformed into one with straight edges (Fig. 3). The order of transformation can be specified independently. If this order is the same as the order of basis function, the element is called isoparametric. If this order is greater or smaller than the order of basis function, the element is called superparametric or subparametric. Based on the transformed tetrahedron, higher order vector interpolatory basis functions are constructed using the method proposed by Graglia *et al.* [34]. First, the zeroth-order vector basis functions are constructed for the tetrahedron. Higher order vector basis functions are then formed by multiplying the zeroth-order ones with the shifted Silvester–Lagrange interpolating polynomial and a normalization factor. As a result, there are $(p+1)(p+3)(p+4)/2$ basis functions and they are complete to the pth order.

When higher order vector basis functions are employed, the volume integral in (1) is evaluated using Gaussian quadrature. The number of integration points is determined adaptively to achieve desired accuracy. The surface integrals in (1) are treated in a similar manner when $\mathbf{r}$ and $\mathbf{r}'$ do not belong to the same element. When they do, the method proposed by Duffy [35] is employed to evaluate the singular integral. To be more specific, the first integral with respect to dS is carried out using Gaussian quadrature. To carry out the second integral with respect to dS', we first divide the source patch into three subtriangles based on the point $\mathbf{r}$. The integration over each subtriangle is then transformed into an integration over a square. This transformation also removes the singularity in the integrand. The integration over the square is finally evaluated using one-dimensional Gaussian–Legendre quadrature.

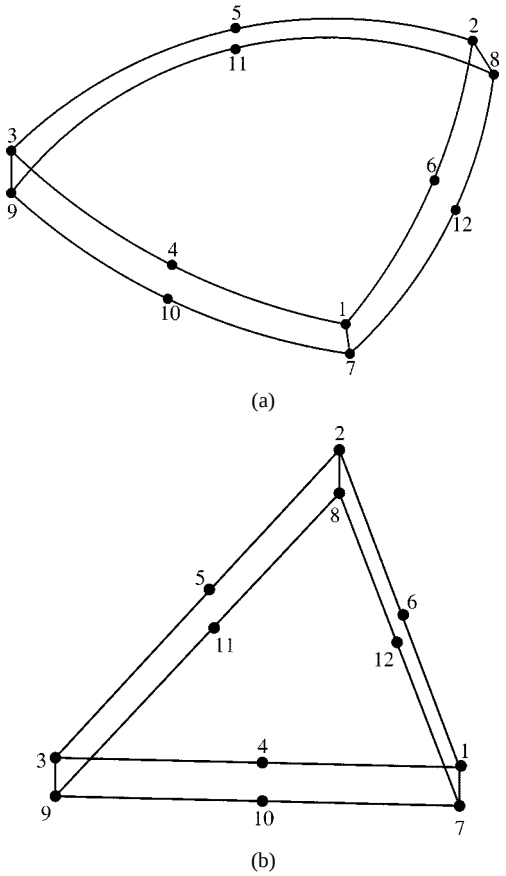

Fig. 8. A mixed second/zeroth-order triangular prism element. (a) Curved element. (b) Rectilinear element.

A computer program is written using higher order tetrahedral elements. The program is structured in such a way that it can use any order of elements. In most FEM applications, the bottleneck is mesh generation, which is always very time consuming and memory intensive. This is particularly true for large problems such as the one treated in this work. To alleviate this difficulty, we recognize that most large cavities such as engine inlets have smooth transition from one section to the other. As a result, we can generate the finite-element mesh layer by layer. If the cavity is empty, we can actually build the entire finite-element mesh using one layer. To be more specific, we first generate the mesh for the bottom layer, whose thickness is only one element. The same mesh is then used for the next layer and the only modification is to slightly adjust the coordinates of each node to conform the cavity geometry.

Next, we present some numerical results to demonstrate the validity and capability of the method. As the first check, we test the self consistency of the method. The first example is a 1.5 λ $\times$

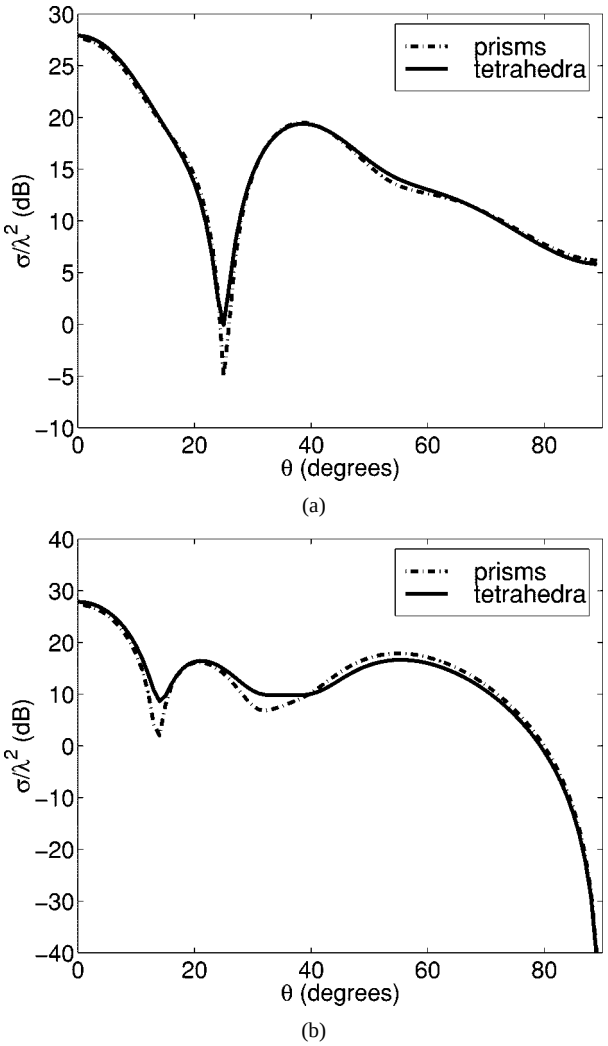

Fig. 9. Monostatic RCS of a 2.0 λ × 2.0 λ × 10.0 λ rectangular cavity. (a) $\theta\theta$ polarization. (b) $\phi\phi$ polarization.

1.5 λ × 0.6 λ rectangular cavity. In this case, the surface of the cavity is flat; hence, there is no issue about geometry modeling. The RCS is given in Fig. 4 as a function of the angle of incidence, obtained by the first-, second-, and third-order elements using the same number of elements (90). The figure demonstrates clearly the convergence with respect to the order of elements. The second example is a circular cavity having a diameter of 0.61λ and depth of 2.1λ. In this case, the surface of the cavity is curved and it is critical to have accurate geometry modeling. The RCS of this cavity is shown in Fig. 5 as a function of the azimuth angle, calculated by the first-, second-, and third-order elements using the same number of elements (427). The exact RCS should be a constant because of the rotational symmetry of the problem. The results show clearly that this is the case when the order of elements increases.

In the third example, we examine the efficiency of higher order elements. The parameter used in this examination is the root-mean-square (RMS) error defined as

$$\mathrm{RMS} = \sqrt{\frac{1}{N_{\mathrm{sample}}} \sum_{i=1}^{N_{\mathrm{sample}}} |\sigma_{\mathrm{ref}} - \sigma_{\mathrm{cal}}|^2} \qquad (4)$$

where σ_{cal} denotes the calculated RCS and σ_{ref} denotes the reference solution, both measured in decibels and N_{sample} is the number of sampling points, which are the angles of incidence here. The reference solution in this case is obtained using the third-order elements with an overly dense mesh, and it does not change anymore when either the order of elements or the mesh density is increased. Fig. 6(a) displays the RMS error in the monostatic RCS of a 1.0 λ × 1.0 λ × 4.0 λ rectangular cavity as a function of the number of unknowns. It is evident that, for the same number of unknowns, the higher order elements produce more accurate results. For a desired accuracy, the number of unknowns required for the higher order elements is smaller than that for lower-order elements. Fig. 6(b) displays the corresponding CPU time. Although the CPU time increases with the order of elements for the same number of unknown, a careful comparison between Fig. 6(a) and (b) indicates that for a given accuracy, the higher order elements consume less CPU time than the lower-order elements. Hence, the higher order elements are both more accurate and efficient than the lower-order ones.

The last example considered using tetrahedral elements is a circular cavity having a diameter of 2.0λ and depth of 10.0λ. Its monostatic RCS is shown in Fig. 7 and the information about the discretization, computer memory, and CPU time is given in Table I. The calculation is carried out on a Digital personal workstation (500-MHz Alpha 21 164 processor). Clearly, the solution converges when the order of elements increases.

V. Mixed-Order Prism Elements

Although the use of higher order tetrahedral elements yields a remarkable improvement in the accuracy and efficiency of the special FEM, the coefficient $(p+1)^2$ in the computational complexity reduces the amount of savings one can achieve in the memory and computing time. However, if we can design a special element that has a higher order interpolation in the transverse plane and a lower order (say the zeroth-order here) interpolation along the depth of a cavity, the computational complexity indicates that for a fixed-size cavity, the memory requirement scales as D_t^4 and the computing time scales as $D_t^6 D_l$, where D_t denotes the mesh density (number of unknowns per wavelength) in the transverse plane and D_l denotes the mesh density (number of unknowns per wavelength) along the depth of the cavity. Since we use a higher order interpolation in the transverse plane, D_t can be reduced. A reduction by a factor of two can reduce the memory requirement by a factor of 16 and the computing time by a factor of 64 and a reduction of mesh density by a factor of three can reduce the memory requirement by a factor of 81 and the computing time by a factor of 729. Although a lower order interpolation is used along the depth of a cavity, an increase in the mesh density along this direction does not increase the memory requirement and increases the computing time only linearly. Clearly, such an element is optimal for the proposed special method and can be implemented on triangular prisms. Compared to the higher order tetrahedral elements, the mixed-order prism elements using the same order and same mesh density in the transverse plane and the zeroth order along the depth reduces the memory requirement by a factor of $(p+1)^2$ and the computing time by a factor of $(p+1)^2 D/D_l$.

TABLE II
COMPARISON BETWEEN HIGHER ORDER TETRAHEDRAL AND MIXED-ORDER PRISM ELEMENTS

Type of Element	Number of Unknowns	Half-Bandwidth	Memory (MB)	CPU Time (s)
3rd-order Tetrahedra	86,600	3,452	63	28,003
3rd/0th-order Prisms	84,500	421	9	1,473

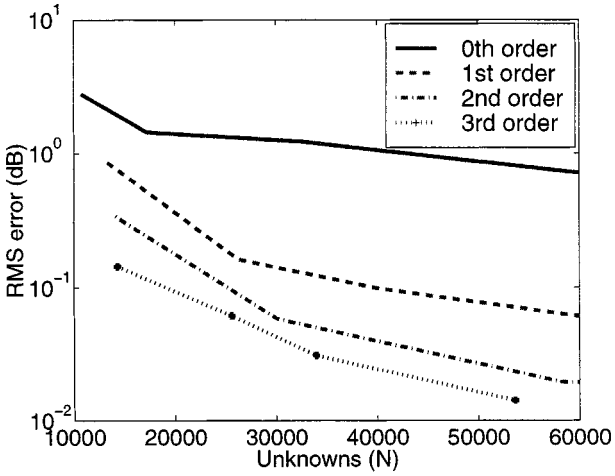

(a)

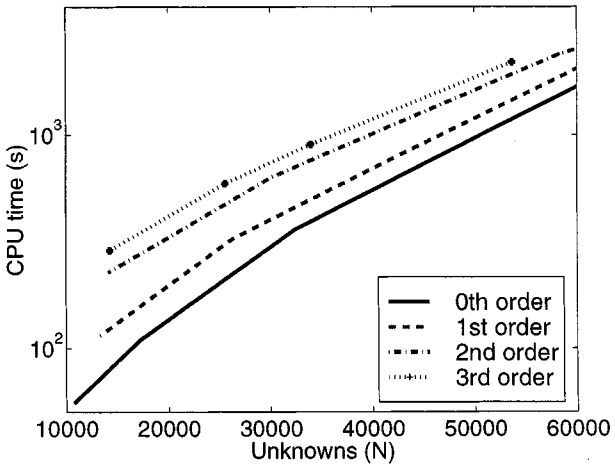

(b)

Fig. 10. (a) RMS error versus the number of unknowns for the monostatic RCS of a 1.5 λ × 1.5 λ × 2.0 λ rectangular cavity modeled with prism elements. (b) Corresponding CPU time.

Similar to the case of tetrahedral element, a curved triangular prism element is first transformed into one with straight edges (Fig. 8). The order of transformation can be specified independently. Since we intend to use higher order basis functions in the transverse plane and lower order ones in the longitudinal direction, the prism element is usually very thin. As a result, we use higher order transformation in the transverse plane and lower order one in the longitudinal direction. The vector basis functions are then constructed by following the approach proposed by Graglia *et al.* [36] with some modifications. The zeroth-order vector basis functions are first constructed. These are then multiplied by the shifted Silvester–Lagrange interpolating polynomial and a normalization factor to form mixed-order vector basis functions. The difference here is that instead of using the same order of interpolation in all directions, we use a higher order in the transverse plane and lower order along the height of the prism. As a result, if we use the pth order in the transverse plane and the zeroth-order in the longitudinal direction, there are $(5p^2+21p+18)/2$ basis functions for each prism.

A computer program is written using the mixed-order triangular prism elements. Again, Gaussian quadrature is employed to perform numerical integration. The surface integrals are dealt with in the same manner as in the case of tetrahedra. For cavities with a smooth variation along the depth, we can again generate the finite-element mesh layer by layer. Because of using prism elements, we actually only need to generate a 2-D triangular mesh. This mesh is then extrapolated in the longitudinal direction to form one layer of elements. As a result, the mesh generation can be accomplished easily and this is the added advantage of using mixed-order triangular prism elements.

To demonstrate the advantage of this type of element, we computed the RCS of a 2 λ × 2 λ × 10 λ rectangular cavity using the third-order tetrahedral elements and the mixed-order prism elements with third-order in the transverse plane and zeroth-order in the longitudinal direction. The number of unknowns in each case was chosen to yield a comparable accuracy (the one using the prism elements is slightly more accurate). The RCS is given in Fig. 9 and the information about the discretization, computer memory, and CPU time is given in Table II. As can be seen, both types of element used about the same number of unknowns. But the mixed-order prism elements have a much smaller half-bandwidth and, hence, use a much smaller memory and CPU time.

Next, we examine the efficiency of mixed-order prism elements with respect to the order in the transverse plane while fixing the one in the longitudinal direction to be zeroth order. The parameter used in this examination is again the RMS error defined in (4). The reference solution is obtained using third-order in the transverse with an overly dense mesh and zeroth-order in the longitudinal direction with a mesh density of 80 points per wavelength. The reference solution so obtained does not change anymore when either the order of elements or the mesh density is increased. For all the calculated results, the mesh density in the longitudinal direction is fixed at 40 points per wavelength so that the accuracy of the results is determined only by the order in the transverse plane. Fig. 10(a) displays the RMS error in the monostatic RCS of a 1.5 λ × 1.5 λ × 2.0 λ rectangular cavity as a function of the number of unknowns. It is evident that for the same number of unknowns, the higher order elements produce more accurate results. For a desired accuracy, the number of unknowns required for the higher order elements

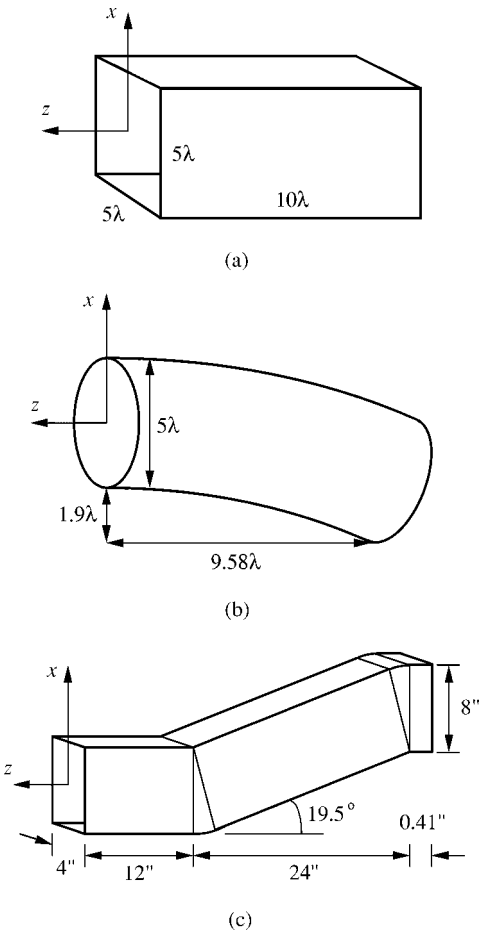

Fig. 11. Three examples. (a) A 5 λ × 5 λ × 10 λ rectangular cavity. (b) A curved circular cavity having a diameter of 5λ and depth of 10.8λ. (c) An offset bend cavity having a total depth of 32λ at 10 GHz.

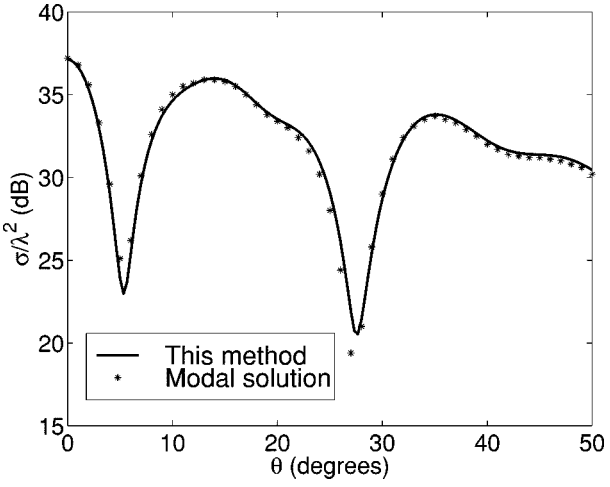

Fig. 12. Monostatic $\theta\theta$-polarized RCS of the rectangular cavity modeled with prism elements.

is much smaller than that for lower order elements. Fig. 10(b) displays the corresponding CPU time. Clearly, for a given accuracy, the higher order elements consume much less CPU time

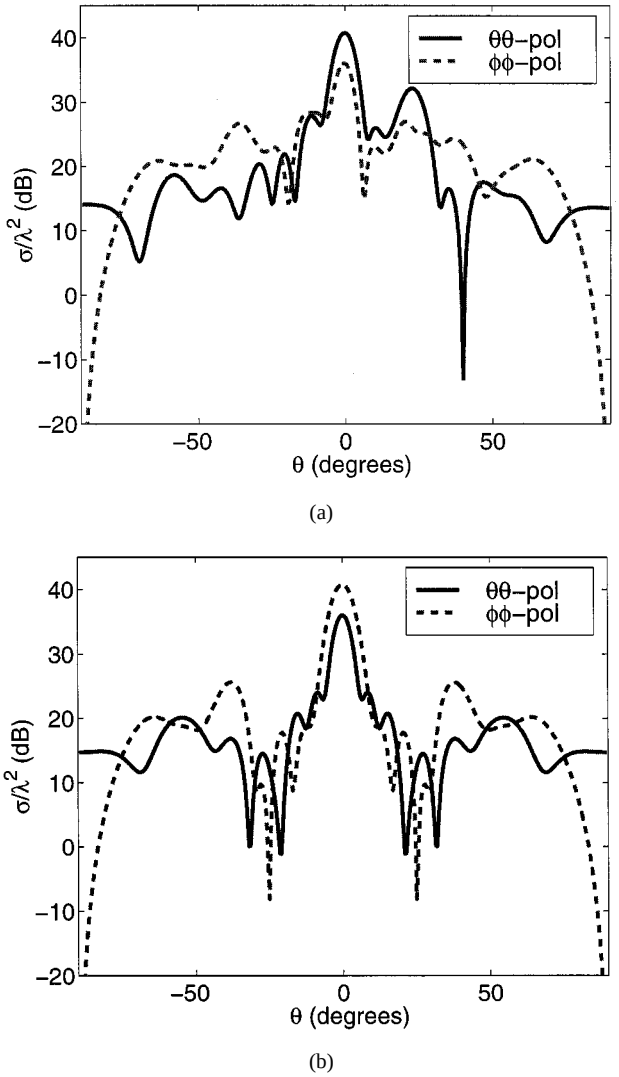

Fig. 13. Monostatic RCS of the curved circular cavity modeled with prism elements. (a) In the xz plane. (b) In the yz plane.

than the lower order elements. Compared to the case of tetrahedra [Fig. 6(b)], here the increase in the CPU time when the order is increased is much less significant.

Finally, we present three examples, all illustrated in Fig. 11, to demonstrate the capability of the proposed method. The first one is a 5 λ × 5 λ × 10 λ rectangular cavity. The computed RCS results are compared with a modal solution [23] in Fig. 12 and excellent agreement is observed. The second is a curved circular cavity having a diameter of 5.0λ. The axis of the cavity is an arc having a radius of 27.5λ and subtends an angle of 22.5°. The results are given in Fig. 13. The third is an offset bend cavity having a total depth of 32λ at 10 GHz. The computed results are compared in Fig. 14 with the measured data and a 2-D solution based on a hybrid boundary integral method and modal approach (BIM/MODE) [24]. For the $\theta\theta$-polarization, our method has a better agreement with the measured data, whereas for the $\phi\phi$-polarization, our solution is very similar to that of the BIM/MODE. For the sake of comparison, the results in Figs. 12 and 14 are calculated for the cavities without the ground plane. All the calculations are done using the mixed third/zeroth-order prism elements. The information about the

TABLE III
INFORMATION ABOUT MEMORY REQUIREMENTS AND CPU TIMES FOR RCS CALCULATIONS

Problem	Number of Unknowns	Half-Bandwidth	Memory (MB)	CPU Time (hr)
Fig. 11(a)	1,354,240	2,645	98	161
Fig. 11(b)	1,014,256	3,373	180	169
Fig. 11(c)	5,365,353	2,793	109	652

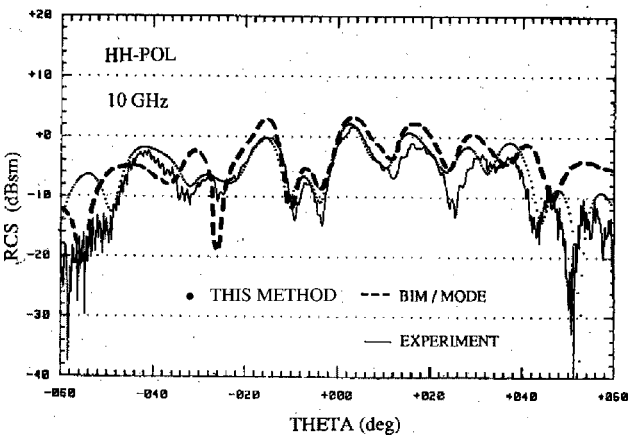

(a)

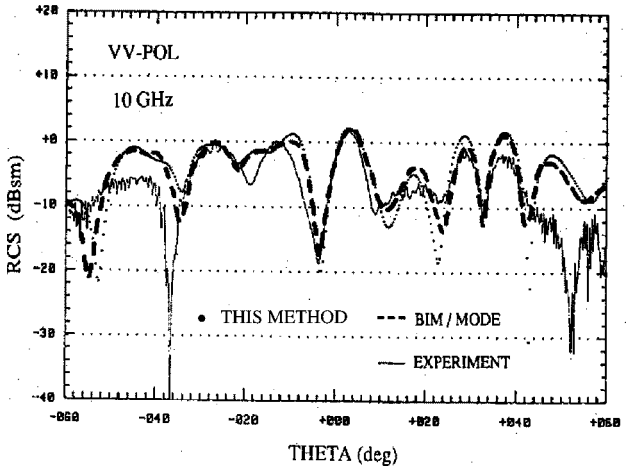

(b)

Fig. 14. Monostatic RCS of the offset bend cavity in the xz plane at 10 GHz modeled with prism elements. (a) $\theta\theta$-polarization. (b) $\phi\phi$-polarization.

number of unknowns, half-bandwidth, memory requirements, and CPU times is given in Table III. The CPU times are measured on a Digital personal workstation (500-MHz Alpha 21 164 processor).

We should note that in all examples presented here, the computations are done without making any assumption on the variation of the cross section of the cavity along its depth. In other words, the computing times would remain the same even if the cavity's cross section varies along its depth. However, if a cavity or some sections of a cavity have a constant cross section, our special algorithm can be modified such that the corresponding computing time is proportional to $\log L$, instead of L, where L is the length of the cavity or the length of the section with a constant cross section, at a cost of increasing the memory requirements by a factor of 1.5. If we utilize this property, the CPU times for the calculation of the three examples in Fig. 11 are reduced to 7.1, 11.8, and 23.7 h, respectively, with the corresponding memory requirements increased to 149, 273, and 166 Mb, respectively.

VI. CONCLUSION

A special higher order FEM was described for the analysis of electromagnetic scattering from a large, deep, and arbitrarily shaped open cavity. This method exploits the unique features of the FEM equations and, more importantly, the unique features of the problem. It is designed in such a manner that it uses minimal memory, which is proportional to the maximum cross section of the cavity and independent of the depth of the cavity and its computation time increases only linearly with the depth of the cavity (or even less if the cavity or some of its sections have a constant cross section). Furthermore, it computes the scattered fields for all angles of incidence without requiring significant additional time. The technique was implemented with higher order tetrahedral and mixed-order prism elements, both having curved sides to allow for accurate modeling of arbitrary geometries. Although both types of element yield a remarkably more accurate and efficient solution for scattering by 3-D cavities, the mixed-order prism is optimal for the proposed special solver. This method, when combined with massively parallel techniques, will lead us to see the light of accurate simulation of scattering by a large and deep cavity, often considered a grand challenge in computational electromagnetics in the RCS community.

Finally, we note that the proposed method can be applied to any problem that is electrically much longer in one dimension than in its other two, such as wave propagation in tunnels for wireless communications.

REFERENCES

[1] H. Ling, R. Chou, and S. W. Lee, "Rays versus modes: Pictorial display of energy flow in an open-ended waveguide," *IEEE Trans. Antennas Propagat.*, vol. AP-35, pp. 605–607, May 1987.
[2] ——, "Shooting and bouncing rays: Calculating RCS of an arbitrarily shaped cavity," *IEEE Trans. Antennas Propagat.*, vol. 37, pp. 194–205, Feb. 1989.
[3] H. Ling, S. W. Lee, and R. C. Chou, "High-frequency RCS of open cavities with rectangular and circular cross sections," *IEEE Trans. Antennas Propagat.*, vol. 37, pp. 645–654, May 1989.
[4] P. H. Pathak and R. J. Burkholder, "Modal, ray and beam techniques for analyzing the EM scattering by open-ended waveguide cavities," *IEEE Trans. Antennas Propagat.*, vol. 37, pp. 635–647, May 1989.
[5] ——, "High-frequency electromagnetic scattering by open-ended waveguide cavities," *Radio Sci.*, vol. 26, pp. 211–218, Jan./Feb. 1991.

[6] R. J. Burkholder and P. H. Pathak, "Analysis of EM penetration scattering by electrically large open waveguide cavities using Gaussian beamshooting," *Proc. IEEE*, vol. 79, pp. 1401–1412, Oct. 1991.
[7] R. J. Burkholder, R. C. Chou, and P. H. Pathak, "Two ray shooting methods for computing the EM scattering by large open-ended cavities," *Comp. Phys. Commun.*, vol. 68, pp. 353–365, 1991.
[8] A. G. Pino, F. Obelleiro, and J. L. Rodriguez, "Scattering from conducting open cavities by generalized ray expansion (GRE)," *IEEE Trans. Antennas Propagat.*, vol. 41, pp. 989–992, July 1993.
[9] F. Obelleriro, J. L. Rodirguez, and R. J. Burkholder, "An iterative physical optics approach for analyzing the electromagnetic scattering by large open-ended cavities," *IEEE Trans. Antennas Propagat.*, vol. 43, pp. 356–361, Apr. 1995.
[10] S. K. Jeng, "Scattering from a cavity-backed slit in a ground plane—TE case," *IEEE Trans. Antennas Propagat.*, vol. 38, pp. 1523–1529, Oct. 1990.
[11] S. K. Jeng and S. T. Tzeng, "Scattering from a cavity-backed slit in a ground plane—TM case," *IEEE Trans. Antennas Propagat.*, vol. 39, pp. 661–663, May 1991.
[12] J. M. Jin and J. L. Volakis, "TE scattering by an inhomogeneously filled aperture in a thick conducting plane," *IEEE Trans. Antennas Propagat.*, vol. 38, pp. 1280–1286, Aug. 1990.
[13] ——, "TM scattering by an inhomogeneously filled aperture in a thick conducting plane," *Proc. Inst. Elect. Eng.*, pt. H, vol. 137, pp. 153–159, June 1990.
[14] ——, "A finite-element boundary integral formulation for scattering by three-dimensional cavity-backed apertures," *IEEE Trans. Antennas Propagat.*, vol. 39, pp. 97–104, Jan. 1991.
[15] ——, "A hybrid finite-element method for scattering and radiation by microstrip patch antennas and arrays residing in a cavity," *IEEE Trans. Antennas Propagat.*, vol. 39, pp. 1598–1604, Nov. 1991.
[16] T. Wang, R. F. Harrington, and J. R. Mautz, "Electromagnetic scattering from and transmission through arbitrary apertures in conducting bodies," *IEEE Trans. Antennas Propagat.*, vol. 38, pp. 1805–1814, Nov. 1990.
[17] T. M. Wang and H. Ling, "A connection algorithm on the problem of EM scattering from arbitrary cavities," *J. Electromagn. Waves Appl.*, vol. 5, no. 3, pp. 301–314, 1991.
[18] ——, "Electromagnetic scattering from three-dimensional cavities via a connection scheme," *IEEE Trans. Antennas Propagat.*, vol. 39, pp. 1505–1513, Oct. 1991.
[19] C. C. Lu and W. C. Chew, "A near-resonance decoupling approach (NRDA) for scattering solution of near-resonant structures," *IEEE Trans. Antennas Propagat.*, vol. 45, pp. 1857–1862, Dec. 1997.
[20] D. D. Reuster and G. A. Thiele, "A field iterative method for computing the scattered electrical fields at the apertures of large perfectly conducting cavities," *IEEE Trans. Antennas Propagat.*, vol. 43, pp. 286–290, Mar. 1995.
[21] C. S. Lee and S. W. Lee, "RCS of a coated circular waveguide terminated by a perfect conductor," *IEEE Trans. Antennas Propagat.*, vol. AP-35, pp. 391–398, Apr. 1987.
[22] A. Altintas, P. H. Pathak, and M. C. Liang, "A selective modal scheme for the analysis of EM coupling into or radiation from large open-ended waveguide," *IEEE Trans. Antennas Propagat.*, vol. 36, pp. 84–96, Jan. 1988.
[23] S. W. Lee and H. Ling, "Data Book for Cavity RCS," Electromagn. Lab., Univ. Illinois, Urbana, IL, Tech. Rep. SWL89-1, Jan. 1989.
[24] H. Ling, "RCS of waveguide cavities: A hybrid integral/modal approach," *IEEE Trans. Antennas Propagat.*, vol. 38, pp. 1413–1419, Sept. 1990.
[25] H. T. Anastassiu, J. L. Volakis, and D. C. Ross, "The mode matching technique for electromagnetic scattering by cylindrical waveguides with canonical terminations," *J. Electromagn. Waves and Appl.*, vol. 9, pp. 1363–1391, Nov./Dec. 1995.
[26] R. G. Layden and C. E. Ryan, "Scattering by over-moded, varying cross-section waveguide," in *IEEE APS Int. Symp. Dig.*, vol. 4, Dallas, TX, May 1990, pp. 1718–1721.
[27] R. Lee and T. T. Chia, "Analysis of electromagnetic scattering from a cavity with a complex termination by means of a hybrid ray-FDTD method," *IEEE Trans. Antennas Propagat.*, vol. 41, pp. 1560–1569, Nov. 1993.
[28] D. C. Ross, J. L. Volakis, and H. T. Anastassiu, "Hydrid finite element-modal analysis of jet engine inlet scattering," *IEEE Trans. Antennas Propagat.*, vol. 43, pp. 277–285, Mar. 1995.
[29] J. M. Jin, S. Ni, and S. W. Lee, "Hybridization of SBR and FEM for scattering by large bodies with cracks and cavities," *IEEE Trans. Antennas Propagat.*, vol. 43, pp. 1130–1139, Oct. 1995.
[30] T. T. Chia, R. J. Burkholder, and R. Lee, "The application of FDTD in hybrid methods for cavity scattering analysis," *IEEE Trans. Antennas Propagat.*, vol. 43, pp. 1082–1090, Oct. 1995.
[31] J. M. Jin, "Electromagnetic scattering from large, deep, and arbitrarily-shaped open cavities," *Electromagn.*, vol. 18, no. 1, pp. 3–34, Jan./Feb. 1998.
[32] R. Lee and A. C. Cangellaris, "A study of discretization error in the finite-element approximation of wave solutions," *IEEE Trans. Antennas Propagat.*, vol. 40, pp. 542–549, May 1992.
[33] J. M. Jin, *The Finite Element Method in Electromagnetics*. New York: Wiley, 1993.
[34] R. D. Graglia, D. R. Wilton, and A. F. Peterson, "Higher order interpolatory vector bases for computational electromagnetics," *IEEE Trans. Antennas Propagat.*, vol. 45, pp. 329–342, Mar. 1997.
[35] M. G. Duffy, "Quadrature over a pyramid or cube of integrands with a singularity at a vertex," *J. Numer. Anal.*, vol. 19, pp. 1260–1262, Dec. 1982.
[36] R. D. Graglia, D. R. Wilton, A. F. Peterson, and I. L. Gheorma, "Higher order interpolatory vector bases on prism elements," *IEEE Trans. Antennas Propagat.*, vol. 46, pp. 442–450, Mar. 1998.

Jian Liu was born in Shanghai, China, on December 9, 1974. He received the B.S. and M.S. degrees in electrical engineering from the University of Science and Technology of China, Anhui, China, in 1995 and 1998, respectively. He is currently working toward the Ph.D. degree in electrical engineering at the University of Illinois, Urbana-Champaign.

Since 1998, he has been a Research Assistant at the Center for Computational Electromagnetics at the University of Illinois, Urbana-Champaign. His current research interests include the numerical analysis of electromagnetic problems using the finite-element and integral equation based methods.

Jian-Ming Jin (S'87-M'89-SM'94) received the B.S. and M.S. degrees in applied physics from Nanjing University, Nanjing, China, in 1982 and 1984, respectively, and the Ph.D. degree in electrical engineering from the University of Michigan, Ann Arbor, in 1989.

He is an Associate Professor of Electrical and Computer Engineering and Associate Director of the Center for Computational Electromagnetics, University of Illinois at Urbana-Champaign. He has authored or coauthored over 90 papers in refereed journals and several book chapters. He has also authored *The Finite Element Method in Electromagnetics* (New York: Wiley, 1993) and *Electromagnetic Analysis and Design in Magnetic Resonance Imaging* (Boca Raton, FL: CRC, 1998), and coauthored *Computation of Special Functions* (New York: Wiley, 1996). His current research interests include computational electromagnetics, scattering and antenna analysis, electromagnetic compatibility, and magnetic resonance imaging. He currently serves as an associate editor of *Radio Science* and is also on the editorial board for *Electromagnetics Journal* and *Microwave and Optical Technology Letters*.

Dr. Jin is a member of Commision B of USNC/URSI, Tau Beta Pi, and International Society for Magnetic Resonance in Medicine. He was a recipient of the 1994 National Science Foundation Young Investigator Award and the 1995 Office of Naval Research Young Investigator Award. He also received a 1997 Xerox Research Award presented by the College of Engineering, University of Illinois at Urbana-Champaign, and was appointed as the first Henry Magnuski Outstanding Young Scholar in the Department of Electrical and Computer Engineering in 1998. He served as an associate editor of the IEEE TRANSACTIONS ON ANTENNAS AND PROPAGATION (1996–1998). He was the symposium cochairman and technical program chairman of the Annual Review of Progress in Applied Computational Electromagnetics in 1997 and 1998, respectively. His name is often listed in the University of Illinois at Urbana-Champaign's *List of Excellent Instructors.*